


B7-H3 and CSPG4 co-targeting as Pan-CAR-T cell treatment of triple-negative breast cancer

Simone Stucchi,¹ Roberto Borea,¹ Susana Garcia-Recio,² Manuela Zingarelli,¹ Patrick D Rädler,² Elena Camerini,¹ Caroline Marnata Pellegry,¹ Siobhan O'Connor,³ H Shelton Earp,¹ Lisa A Carey,⁴ Charles M Perou,² Barbara Savoldo,^{1,5} Gianpietro Dotti ^{1,6}

To cite: Stucchi S, Borea R, Garcia-Recio S, *et al.* B7-H3 and CSPG4 co-targeting as Pan-CAR-T cell treatment of triple-negative breast cancer. *Journal for ImmunoTherapy of Cancer* 2025;**13**:e011533. doi:10.1136/jitc-2025-011533

► Additional supplemental material is published online only. To view, please visit the journal online (<https://doi.org/10.1136/jitc-2025-011533>).

Accepted 12 May 2025

ABSTRACT

Purpose Chimeric antigen receptor T (CAR-T) cell therapy is under clinical investigation in patients with metastatic triple-negative breast cancer (TNBC). However, the identification of targetable antigens remains a high priority to avoid toxicity and prevent tumor escape.

Experimental design Here we analyzed the gene expression of B7-H3 (*CD276*) and chondroitin sulfate proteoglycan 4 (*CSPG4*) in 98 TNBC samples identified in the AURORA US Network and Rapid Autopsy RNA sequencing data set at University of North Carolina (UNC). We then performed immunohistochemistry analysis for B7-H3 and CSPG4 protein expression in 151 TNBC samples collected at UNC. Finally, the validity of the proposed B7-H3 and CSPG4 co-targeting was tested in clinically relevant TNBC patient derived xenograft (PDX) models.

Results We observed that *CD276* and *CSPG4* genes are broadly and comparably expressed in TNBC samples, and gene expression is generally conserved in tumor metastases. None of the TNBC analyzed met the criteria for simultaneous low expression of *CSPG4* and *CD276* genes. Immunohistochemistry analysis showed a median H-score of 138 (105–168, lower and upper quartile, respectively) for B7-H3 expression and a median H-score of 33 (14–78 lower and upper quartile, respectively) for CSPG4 expression. Notably, 49% of the TNBC cores with B7-H3 H-score ≤105 exhibited a CSPG4 H-score exceeding its median value, and 37% and 18% of the TNBC cores with low B7-H3 expression scored CSPG4 expression above its median H-score or exceeded its upper quartile, respectively, confirming that at least one of these two proteins is expressed in 94% of the analyzed tumors. Finally, optimized dual-specific B7-H3 and CSPG4 CAR-T cells eradicated tumors with mixed antigen expression in TNBC PDX models.

Conclusions These data highlight the clinical potential of the proposed approach that could be applicable to the great majority of patients with TNBC as well as most of patients with breast cancer in general.

INTRODUCTION

Triple-negative breast cancer (TNBC) is characterized by the absence of endocrine receptors, HER2 overexpression and gene amplification, and is predominantly

WHAT IS ALREADY KNOWN ON THIS TOPIC

⇒ Chimeric antigen receptor T (CAR-T) cell therapy is clinically explored in triple-negative breast cancer (TNBC) and effective and safe targets remain to be defined.

WHAT THIS STUDY ADDS

⇒ Here we report in a large cohort of TNBC samples a systematic analysis of the expression of B7-H3 and chondroitin sulfate proteoglycan 4 (CSPG4).

HOW THIS STUDY MIGHT AFFECT RESEARCH, PRACTICE OR POLICY

⇒ Here we indicate that targeting B7-H3 and CSPG4 simultaneously would provide CAR-T cells preventing tumor escape.

identified as the molecularly basal-like (BL) subtype (75–80%) in the context of the molecular characterization of breast cancer (BC).^{1–4} TNBC accounts for 15–20% of all BC, among which it has the poorest prognosis and limited therapeutic options. The combination of immune checkpoint inhibitors and chemotherapy has improved the clinical outcome of TNBC.^{5,6} However, the relapse rate remains high, and patients with metastatic disease experience either primary or secondary resistance, supporting the need for new treatments. To this end, one strategy is the adoptive transfer of engineered T cells such as chimeric antigen receptor T (CAR-T) cells.

The identification of suitable antigens for CAR-T cell therapy in solid tumors remains a priority to ensure both safety and efficacy. Self-antigens overexpressed by tumor cells with low expression in normal tissues such as carcinoembryonic antigen, mesothelin, MUC1, NKGD2 ligands, ROR1, CD70 and c-Met have been proposed as targets for TNBC, and c-Met and ROR1 specific CAR-T



© Author(s) (or their employer(s)) 2025. Re-use permitted under CC BY-NC. No commercial re-use. See rights and permissions. Published by BMJ Group.

For numbered affiliations see end of article.

Correspondence to

Dr Gianpietro Dotti;
gdotti@med.unc.edu

cells have been clinically tested, but with modest activity.⁷⁸ One of the reasons for the modest activity of CAR-T cells in solid tumors, including TNBC, is the heterogeneous expression of target antigens that causes rapid tumor escape.^{9–11} Targeting more than one antigen with optimally designed CAR molecules is one of the strategies proposed to prevent tumor escape.^{12–14}

Systematic analyses of the expression of antigens that can be co-targeted with CAR-T cells to control both primary and metastatic lesions in TNBC are lacking. B7-H3 is a type I transmembrane protein that belongs to the B7 family,¹⁵ and it is aberrantly expressed in several solid tumors, while limited expression is seen in normal tissues.^{16–17} We and others have previously generated B7-H3.CAR-T cells and found that they control the growth of multiple solid tumors in vitro and in vivo.^{18–20} In a small series of 74 BC samples, B7-H3 protein has been detected in 56% of the primary lesions with weak expression in adjacent tissues.²¹ In another cohort of 25 BC samples, all samples showed B7-H3 expression, with 40% of the samples showing strong positivity.²² Lee and colleagues reported the expression of B7-H3 in both epidermal growth factor receptor HER3⁺ (52%) and HER3[−] (62%) BC samples.²³ Similarly, the transmembrane proteoglycan chondroitin sulfate proteoglycan 4 (CSPG4) is overexpressed in a variety of human malignancies, and it is involved in tumor proliferation and metastatic progression by facilitating tumor cell interactions with the extracellular matrix.²⁴ CSPG4 is also expressed in pericytes of the tumor vasculature, further underlining its multifaceted role in tumor progression.^{25–26} We previously reported that CSPG4 is not expressed in normal tissues^{26–27} and that the MDA-MB-231 tumor cell line, which is an aggressive TNBC cell line, can be targeted with CSPG4.CAR-T cells.²⁷ A previous report in a small series of 44 BC samples indicated that CSPG4 protein is overexpressed in 72% of tumors.²⁸ Similarly, Hu and colleagues reported that 60% of the 85 TNBC samples analyzed by immunohistochemistry showed high expression of CSPG4.²⁹

Here, we report the systematic analysis of the expression of the *CD276* and *CSPG4* genes in 98 TNBC samples (AURORA US Network cohort and University of North Carolina (UNC) Rapid Autopsy Program cohort)³⁰ compared with other molecular subsets of BC and including both primary and metastatic lesions. We then report B7-H3 and CSPG4 protein expression by immunohistochemistry in 151 samples of TNBC. Finally, we show in clinically relevant TNBC patient derived xenograft (PDX) models that optimized CAR-T cells co-targeting B7-H3 and CSPG4 could represent an effective CAR-T cell therapy applicable to the great majority of patients with TNBC and other BC types.

MATERIAL AND METHODS

Cell lines

The TNBC tumor cell line MDA-MB-231 was obtained from the German Collection of Microorganism and

Cell Cultures GmbH (DSMZ, ACC 732), while SUM-159, 293T and RAJI were obtained from American Type Culture Collection (ATCC). All cells were maintained in culture with the appropriate media, either Roswell Park Memorial Institute (RPMI)-1640 (Gibco) or Dulbecco's Modified Eagle Medium (DMEM) (Gibco), supplemented with 10% fetal bovine serum (FBS) (Cytiva), 1% GlutaMAX (Gibco), and 1% penicillin/streptomycin (Gibco) in a humidified atmosphere (5% CO₂) at 37°C. All cell lines were routinely tested to confirm the absence of *Mycoplasma* contamination and assessed for the expression of tumor markers by flow cytometry to confirm identity. Cells were kept in culture for less than three consecutive months. The TNBC PDX WHIM12, WHIM2, and WHIM30 were previously characterized into three different subtypes based on PAM50 and “Nine-cell line Claudin-Low predictor”, with WHIM12 being classified as claudin-low (CL), and WHIM2 and WHIM30 as BL/TNBC.^{31–33} WHIM12 is the only PDX that can be expanded ex vivo. We used this PDX to generate WHIM12 B7-H3^{KO} and WHIM12 CSPG4^{KO} cells using the CRISPR-Cas9 technology (sgRNA for B7-H3 (TTCAGGGACCTGGACCTCCA, IDT) and sgRNA for CSPG4 (TGTGGAGCAATACGGTACCC, ITD). To obtain a 100% KO efficiency for B7-H3 and CSPG4 cells were sorted using the MACSQuant Tyto Cell Sorter (Miltenyi Biotec).

Generation of retroviral vectors and CAR-T cells

B7-H3.CAR and CSPG4.CAR have been previously described.^{18–34} The inducible caspase-9 safety switch (iC9) was included in the B7-H3.CAR cassettes using a 2A sequence and cloned into the SFG retroviral vector as previously described.^{18–35} Dual CARs encoding both B7-H3 and CSPG4 specific CARs were constructed to encode the CD28 or 4-1BB costimulatory endodomains in trans and to share one single CD3ζ chain.¹⁴ Retroviral supernatants used to transduce human T cells were prepared as previously described.³⁶ For the generation of CAR-T cells, peripheral blood mononuclear cells (PBMCs) were isolated from buffy coats of healthy donors (Gulf Coast Regional Blood Center, Houston, Texas, USA) by Lymphoprep (Accurate Chemical and Scientific Corporation) density-gradient centrifugation. PBMCs were activated with agonistic CD3 (Miltenyi Biotec) and CD28 (Becton Dickinson, Mountain View, California, USA) antibodies (Abs) in complete media RPMI 1640 hyclone (Cytiva) 45%, Click medium (Irvine Scientific, Santa Ana, California, USA) 45%, supplemented with 10% FBS and 1% L-glutamine, and 1% penicillin/streptomycin, transduced and expanded in the presence of interleukin (IL)-7 (10 ng/mL, PeproTech) and IL-15 (5 ng/mL, PeproTech) as previously described.³⁷ Cells were expanded for up to 12–14 days and used for in vitro and in vivo experiments.

Flow cytometry

We performed flow cytometry using Abs specific to human CD276, CD3, CD8, CD19, CD45, CD45RA, CD69, CCR7, PD-1, TIM3, LAG3, CTLA-4, CD62L and CD45RO

(all from BD) and NG2 (CSPG4, from Miltenyi), conjugated with BV421, BV510, BV605, BV711, FITC, AF488, PE, PE-Cy7, PE, FITC, APC or APC-Cy7 fluorochromes. Expression of the B7-H3.CAR was detected using the recombinant human B7-H3-Fc chimeric protein (R&D) and the secondary goat anti-Human IgG (H+L, Jackson Lab) Ab, while CSPG4.CAR was detected using a specific anti-idiotypic Ab followed by staining with a secondary goat anti-mouse Ab (BD Biosciences).³⁴ Samples were acquired with a BD LSR Fortessa using the BD FACS Diva software (BD Biosciences). For each sample, a minimum of 10,000 events were acquired. Data analyses were performed with the FlowJo V.10 software (BD Biosciences). B7-H3 and CSPG4 antigen expression was also assessed using 376.96 and 763.74 Abs derived from specific hybridomas, respectively, and a secondary goat anti-mouse Ab as previously described.^{18,34} B7-H3 and CSPG4 antigen density in tumor cells was measured using QIFIKIT (Agilent) according to the manufacturer's instructions.

Co-culture experiments

Tumor cells and T cells were plated at different effector to target (E:T) ratios (1:2 to 1:5) in the absence of exogenous cytokines. Cells were collected after 5 days (for ratio 1:2) and 7 days (for ratio 1:5) of culture, and tumor cells and T cells were quantified using CD276 (B7-H3), NG2 (CSPG4) or CD19 (Raji tumor cells) and CD3 Abs, respectively. Zombie Aqua Fixable Viability Dye (BioLegend) was used to exclude dead cells. Cell numbers were quantified using CountBright Absolute Counting Beads (Thermo Fisher Scientific). Supernatants were collected after 24 hours to measure IL-2 and interferon (IFN)- γ using specific ELISA kits (R&D system) following the manufacturer's instructions and a Synergy2 microplate reader (BioTek) with Gen5 software (BioTek).

Patient-derived TNBC xenograft (PDX) model

Female or male 6–8 weeks old NSG mice were obtained from the Animal Core Facility at UNC. Mice were housed in the Animal Core Facility at UNC. All mouse experiments were performed in accordance with UNC Animal Husbandry and Institutional Animal Care and Use Committee (IACUC) guidelines and were approved by the UNC IACUC. PDX WHIM12, WHIM2, and WHIM30 were expanded in vivo in NSG mice. For the in vivo experiments, PDXs were collected from tumor-bearing mice and single tumor cell suspension was obtained using the human tumor dissociation kit (Miltenyi Biotec). Between 0.1×10^6 and 1×10^6 tumor cells were injected orthotopically into the mammary fat pad. Tumor growth was measured two times a week using caliper measurements. Tumor-bearing mice were treated by day 14–21, depending on the kinetic of tumor growth, with either control/non-transduced (NT) T cells or CAR-T cells, which were administered by tail vein injection. Tumor volume was calculated using the formula ($V = 0.5 \times L \times W^2$). Mice were monitored twice a week and euthanized according to UNC-IACUC standards when tumor measurement

reached the volume of 1.2 cm^3 or if mice had a body condition score equal to or below 2. Mice that cleared the tumor after CAR-T cell treatment were euthanized after 92, 84, and 95 days post WHIM12, WHIM2 and WHIM30 tumor injection, respectively. Mice that received the WHIM12 B7-H3^{KO} and WHIM12 CSPG4^{KO} cells and controlled the tumor growth after CAR-T cell treatment were euthanized on day 113 post-tumor injection. Blood and bone marrow were collected at the endpoint for analysis by flow cytometry.

Gene expression analysis of RNA sequencing data

RNA expression of B7-H3 (CD276) was assessed in two previously published cohorts: 123 tumor samples from the AURORA US Network and 82 tumor samples from the UNC Rapid Autopsy Program (dbGAP (phs001866) and GEO (GSE147322)).³⁰ We merged the dataset following the previously described methodology.³⁰ Briefly, the upper quarter normalized and log2-transformed data from the two datasets was merged. To improve the batch effect between the two data types (formalin fixed paraffin embedded (FFPE) and formalin fixed (FF)), we used the *removeBatchEffect* function from the limma R package, including both batches in the formula.³⁸ To minimize the false-positive results due to the normal tissue contamination, we followed the same steps as in the AURORA US.³⁰ We removed 1,451 genes of the “normal-like tissue signature” used in this publication from the data matrix of the 205 AURORA-UNC cohort.³⁰ To avoid the possible confounding factor of intrinsic molecular subtype in the subsequent analysis, in some of these analyses, we divided tumors into two datasets based on the subtype of the primary tumor from each pair: a “Lums-HER2E set” comprising all LumA, LumB and HER2E subtype participants also referred to as the “Luminal” group and a “Basals set” containing BL subtype participants only.

Immunohistochemistry of human tissue microarrays

Immunohistochemistry (IHC) was carried out in the Leica Bond-Rx fully automated staining platform (Leica Biosystems, Norwell, Massachusetts, USA). Slides were dewaxed in Bond Dewax solution (AR9222) and hydrated in Bond Wash solution (AR9590). Epitope retrieval for both targets was performed for 20 min in Bond-epitope retrieval solution 1 pH 6.0 (AR9661). The epitope retrieval was followed by 5 min endogenous peroxidase blocking using Bond peroxide blocking solution (DS9800) and 10 min protein blocking. Slides were incubated with CSPG4-specific antibody (1:100; rabbit polyclonal anti CSPG4 (NG2) #ab83178, Abcam, Cambridge, Massachusetts, USA) for 30 min and 1 hour with B7-H3 antibody (1:100; Rabbit monoclonal antibody against CD276 (B7-H3) (clone D9M2L, # 14 058S, Cell Signaling Technology, Inc. Danvers, MA #140585). Detection was done using the Bond Polymer Refine kit (DS9800) with the 3,3'-diaminobenzidine visualization and hematoxylin counterstain. Stained slides were dehydrated and coverslipped. Positive and negative (omitted primary) controls were

included for each staining. Slides were digitally imaged in the Aperio ScanScope AT2 (Leica Biosystems, Norwell, Massachusetts, USA) using 20× objective. Tissue microarrays (TMA) slides were de-arrayed to visualize individual cores using TMA Lab (Aperio). TMA was analyzed blindly by an experienced pathologist. The percentage of positive cells at each intensity level was used to calculate the H-score using the formula: $H\text{-score} = (\% \text{ at } 1+) \times 1 + (\% \text{ at } 2+) \times 2 + (\% \text{ at } 3+) \times 3$.

Statistical analyses

Measurements were summarized as mean±SD. Analysis of variance (one-way) with Tukey's correction was used for comparison of three or more groups, while unpaired Student's t-test was used to compare two groups. Statistical significance was defined at $p < 0.05$. Statistical analysis was performed with Prism V.9 (GraphPad Software) and RStudio V.2024.09.0+375 (<http://cran.r-project.org>).

RESULTS

B7-H3 is expressed in primary and metastatic lesions of TNBC

We assessed the expression of the *B7-H3* (*CD276*) gene in a combined cohort of 205 BC primary tumors (123 samples from the AURORA US Network cohort and an additional 82 tumor samples from the UNC Rapid Autopsy Program cohort).³⁰ 98 samples were identified as TNBC, and these samples clustered mostly in the BL molecular subtype (75–80%), although about 20% of the cases exhibited different molecular signature, including luminal A (LumA), luminal B (LumB), CL, and HER2-enriched (HER2-E).^{1,2,4} TNBC samples showed consistent expression of *CD276* messenger RNA (mRNA) across primary and metastatic samples (figure 1A). When evaluating all BC tumors together, *CD276* mRNA expression was maintained between primary and metastatic samples, without a statistically significant difference (figure 1B). Further stratification by site of metastasis in all tumors showed no significant differences in expression, though a downward trend was observed in liver, lung, and brain metastases compared with primary tumors (figure 1C). Among the combined dataset divided by intrinsic molecular subtypes, *CD276* mRNA expression levels were significantly higher in CL tumors, compared with BL tumors and luminal-like tumors (LumA, LumB) (online supplemental figure S1A). To evaluate organ-specific patterns of *CD276* mRNA expression and minimize potential confounding from intrinsic subtype, we analyzed tumors grouped in two additional ways: BL tumors (online supplemental figure S1B), and Lums-HER2E tumors (LumA, LumB, and HER2E, also referred to as “Luminal” group) (online supplemental figure S1C). Grouping tumors by subtype, the expression of *CD276* mRNA was maintained between primary sites and metastatic sites in all BL tumors (online supplemental figure S1D), but was significantly lower in metastatic tumors compared with their breast counterparts in the luminal group (online supplemental figure S1E). Overall, these data suggest that *CD276* mRNA

expression is broadly preserved between primary and metastatic tumors.

The expression of B7-H3 was then evaluated by immunohistochemistry in 159 cores of TNBC identified among a cohort of 775 cores of BC. The median H-score for B7-H3 expression in TNBC was 138 (105–168, lower and upper quartile, respectively) (figure 1D) and was similar to what was observed for the other 616 BC samples (139 median, 104–162, lower and upper quartile, respectively) (online supplemental figure S1F). In TNBC, B7-H3 was strongly expressed (3+ in ≥20% of the cells) in 16 cores (10%), and at medium levels (2+ in ≥20% of the cells) in other 107 cores (67%). Overall, 123 (77%) cores had medium and/or high B7-H3 expression, with only 12 (8%) cores showing <20% of B7-H3 expression (at any level) (figure 1E,F). As previously reported,¹⁶ B7-H3 was not expressed in normal breast tissues. In summary, these data indicate that B7-H3 is expressed in TNBC in both primary and metastatic lesions and support the rationale for targeting B7-H3 via CAR-T cells in patients with TNBC.

CAR-T cells targeting B7-H3 have cytotoxic activity against TNBC in vitro

We constructed two retroviral cassettes in which the B7-H3. CAR encoding either the CD28 endodomain (CD28ζ) or the 4-1BB endodomain (41BBζ) were coexpressed using a 2A-like sequence with the inducible iC9 safety switch (iC9) that allows the elimination of CAR-T cells in case of toxicity (figure 2A).^{35,39} CD28ζ and 41BBζ CARs were expressed in transduced T cells (figure 2B,C), and CAR-T cells expanded in vitro (figure 2D). B7-H3.CAR-T cells exhibited comparable composition in effector and memory subsets, defined by the expression of CCR7 and CD45RA (figure 2E), and similar expression of the T-cell immunoglobulin and mucin-domain containing-3 (TIM3), lymphocyte activation gene 3 (LAG3), cytotoxic T-lymphocyte associated protein 4 (CTLA-4) and programmed cell death protein 1 (PD-1) markers (figure 2F). The iC9 safety switch was equally functional in CD28ζ and 41BBζ B7-H3.CAR-T cells, with more than 85% of CAR-T cells eliminated after exposure to the chemical inducer of dimerization that activates iC9³⁵ (figure 2G and online supplemental figure S2A). We assessed the effector function of B7-H3.CAR-T cells against two established TNBC tumor cell lines (SUM159 and MDA-MB-231) that express B7-H3 (online supplemental figure S2B). B7-H3.CAR-T cells effectively lysed these TNBC cell lines when tested in a standard 6 hours ⁵¹Cr-release assay (online supplemental figure S2C,D), and showed antitumor effects in co-culture experiments in which CAR-T cells were seeded at different ratios with SUM159 (figure 2H,I) or MDA-MB-231 (figure 2K,L) cells. B7-H3.CAR-T cells also expanded in response to B7-H3 expressing tumor cells (figure 2J,M). No antitumor activity was observed when B7-H3.CAR-T cells were cultured with tumor cells lacking B7-H3 expression (online supplemental figure S2E–G). Supernatants collected from the co-culture experiments showed that B7-H3.CAR-T cells, but not control T cells,

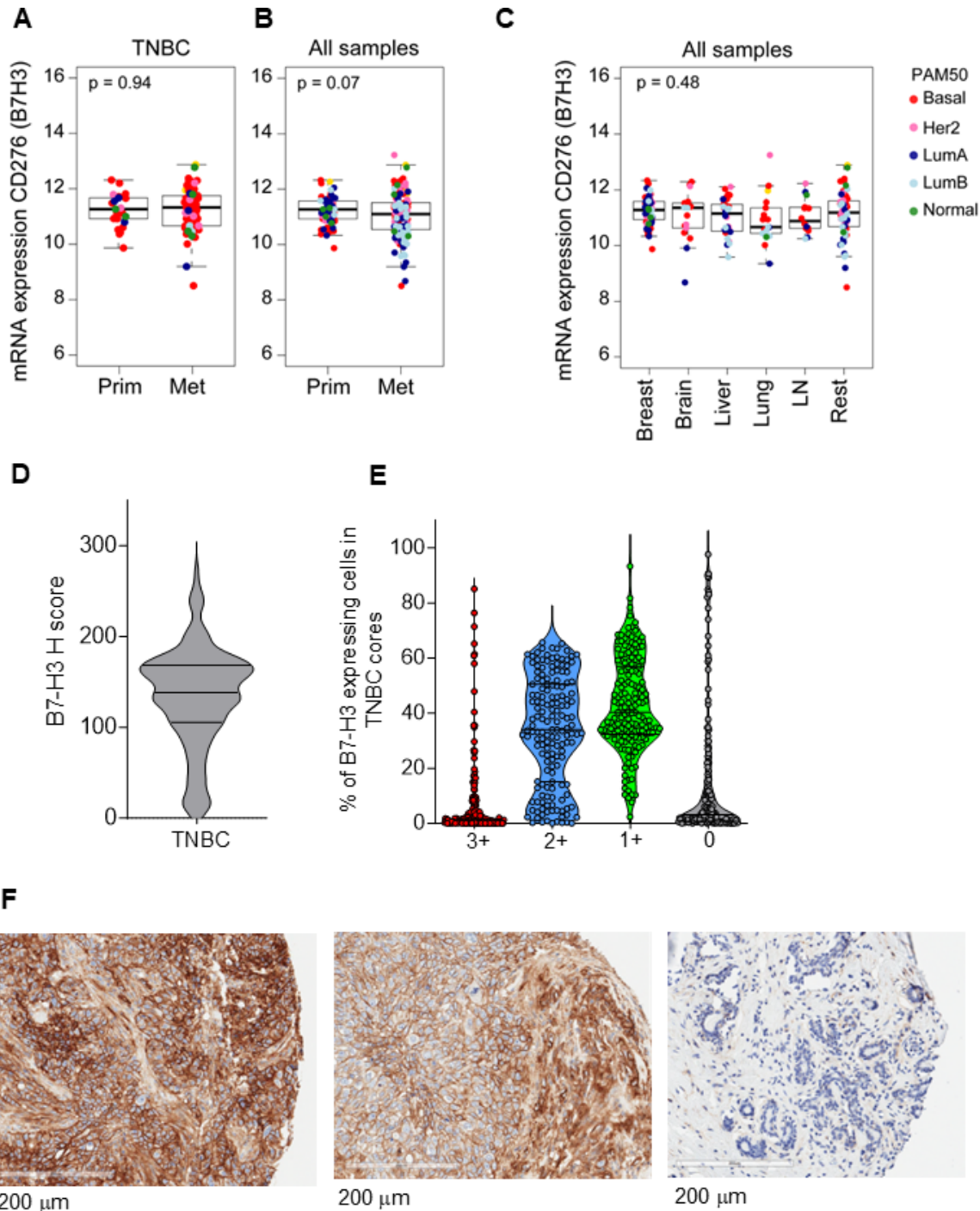


Figure 1 B7-H3 (*CD276*) gene and protein expression in TNBC. (A) *CD276* mRNA expression in 98 TNBC samples in a combined set of 205 breast cancer samples, consisting of 64 primary tumors and 141 metastatic lesions. (B) *CD276* mRNA expression across all samples combined (shown primary tumors vs metastases) (TNBC=98, ER⁺/HER2⁺=76, HER2⁺=34). (C) *CD276* mRNA expression across all samples, stratified by the most common metastatic sites. All box and whisker plots of the figure display the median value on each bar, showing the lower and upper quartile range of the data (Q1–Q3). The whiskers represent the lines from the minimum value to Q1 and Q3 to the maximum value. All comparisons between more than two groups were performed by analysis of variance with a post hoc Tukey test (one-sided). The p values for the post hoc test are shown. A comparison between only two groups was performed using an unpaired t-test (two-sided). mRNA expression is shown as a relative expression of log2 transformed batch-corrected data. (D) Violin plot showing the B7-H3 H-score in 159 TNBC cores by immunohistochemistry staining. Shown is median, lower and upper quartile. (E) Representation of cells in each TNBC core expressing B7-H3 at high (3+), moderate (2+), low (+1) level or not expressing B7-H3 (0). (F) Immunohistochemistry staining for B7-H3 of two representative TNBC cores with H-score 247 (left image) and H-score 194 (middle image), and of a normal breast (right image). Bars represent 200 μ m (magnification 20 \times ; images captured using Aperio ImageScope). LN, lymph node; LumA, luminal A; LumB, luminal B; Met, metastatic tumor; mRNA, messenger RNA; normal, normal-like; Prim, primary tumor; Rest, other sites of metastasis; TNBC, triple-negative breast cancer.

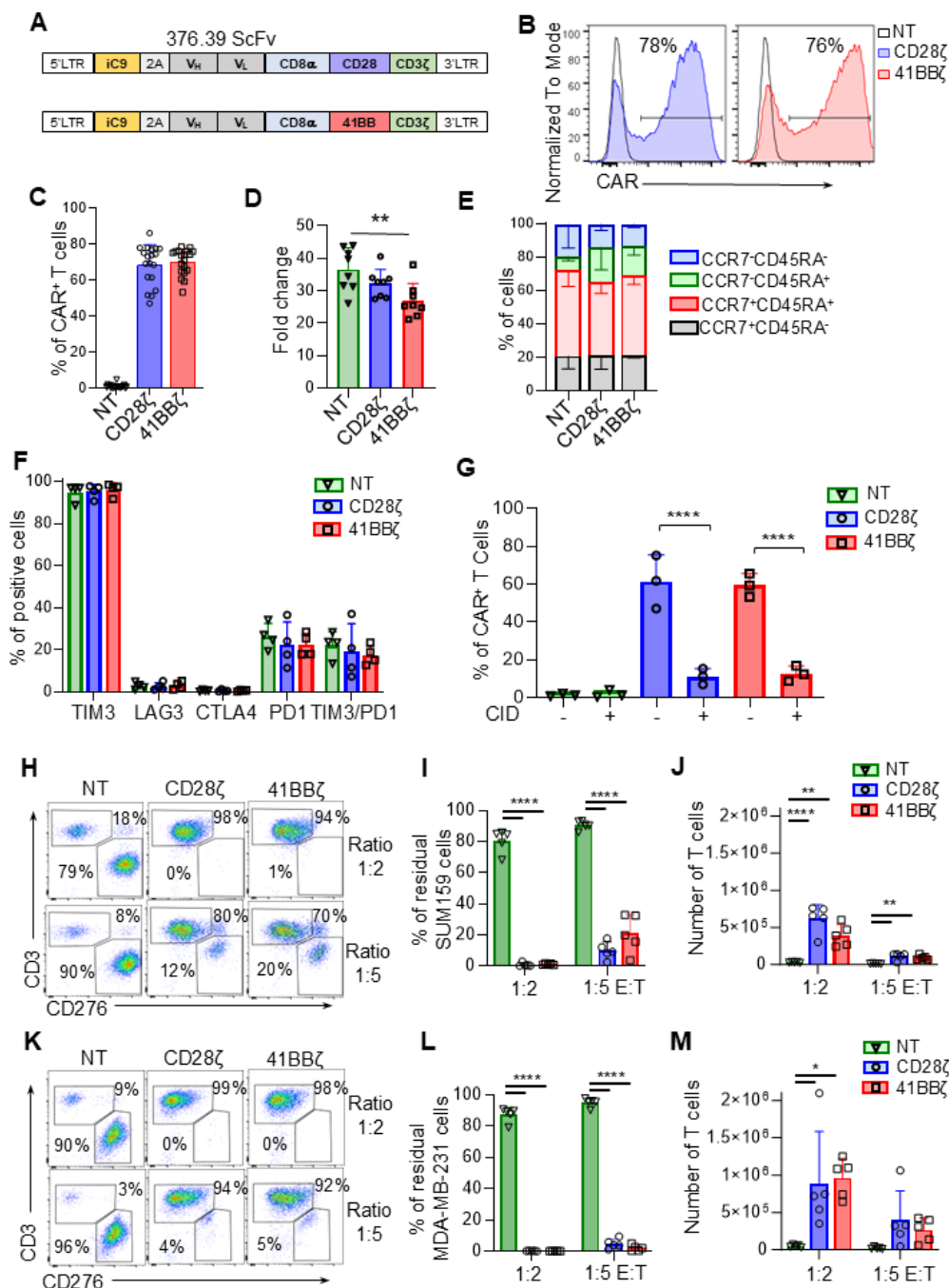


Figure 2 B7-H3.CAR-T cells target TNBC cells in vitro. (A) Schematic representation of retroviral vectors encoding the B7-H3. CAR with either the CD28 and CD3 ζ endodomains (CD28 ζ), or 41BB and CD3 ζ endodomains (41BB ζ). Both vectors encode the iC9 safety switch gene. (B, C) Representative flow cytometry histograms (B) and summary (C) of the B7-H3.CAR expression in transduced T cells. NT indicates control non-transduced T cells; n=19; data represent mean \pm SD. (D) T-cell expansion at day 10 of culture expressed as fold changes; n=8, data represent mean \pm SD, **p=0.0057 by one-way ANOVA with Tukey's correction. (E, F) Phenotypic characterization of B7-H3.CAR-T cells based on CCR7 and CD45RA expression (E) and TIM3, LAG3, CTLA-4 and PD-1 expression (F) at day 10 of culture; n=4, data represent mean \pm SD. (G) Representative flow cytometry histograms showing B7-H3.CAR-T cells surviving 24 hours after exposure to chemical inducer of dimerization 0.5 nM that activates the iC9 gene; n=3, data represent mean \pm SD, ****p<0.0001 by one-way ANOVA with Tukey's correction. (H–M) TNBC SUM159 (H–J) and MDA-MB-231 (K–M) cell lines were co-cultured with B7-H3.CAR-T cells or control non-transduced T cells (NT) at 1:2 or 1:5 effector to target (E:T) ratios. After 5 days, T cells (CD3 $^{+}$) and tumor cells (B7-H3 $^{+}$) were collected and enumerated by flow cytometry. Representative flow cytometry plots (H) and summary of residual tumor cells (I) and T cells (J) for SUM159 co-culture experiments; n=5, data shown are mean \pm SD, ****p<0.0001, **p=0.0033, *p=0.0332 by one-way ANOVA with Tukey's correction. Representative flow plots (K) and summary of residual tumor cells (L) and T cells (M) of MDA-MB-231 co-culture experiments; n=5, data shown as mean \pm SD, ****p<0.0001, *p=0.0228 by one-way ANOVA with Tukey's correction. ANOVA, analysis of variance; CAR, chimeric antigen receptor; iC9, inducible caspase-9; PD-1, programmed cell death protein 1; scFv, single chain variable fragment; TIM3, T-cell immunoglobulin and mucin-domain containing-3; TNBC, triple-negative breast cancer.

released IFN- γ and IL-2 in response to tumor cells (online supplemental figure S2H–O). Overall, these data support the ability of B7-H3.CAR-T cells encoding either CD28 or 4-1BB endodomain to eliminate TNBC cells in vitro, while maintaining the iC9 function.

CAR-T cells targeting B7-H3 eliminate PDX TNBC in vitro and in vivo

We tested three TNBC PDX models (WHIM12, WHIM2, and WHIM30) with WHIM12 being classified as CL TNBC, and WHIM2 and WHIM30 as BL TNBC^{31–33} (online supplemental figure S3A). We confirmed the expression of B7-H3 in these PDX using flow cytometry on cells collected from tumor-bearing NSG mice (online supplemental figure S3B). Since WHIM12 cells grow in vitro, we ensured that B7-H3.CAR-T cells targeted this PDX (online supplemental figure S3C–J). Next, we assessed the antitumor effects of B7-H3.CAR-T cells in vivo by engrafting NSG mice with WHIM12, WHIM2, or WHIM30 PDX. On orthotopic tumor engraftment on day 21 for WHIM12 (tumor volume = 0.19 ± 0.04 cm³) and WHIM30 (tumor volume = 0.03 ± 0.01 cm³), and on day 14 for WHIM2 (tumor volume = 0.04 ± 0.01 cm³) (online supplemental figure S4A) mice received either control NT T cells, CD28 ζ or 41BB ζ B7-H3.CAR-T cells (5×10^6 cells) by intravenous injection. In all PDX models, tumors grew in mice receiving control NT T cells. In contrast, tumors decreased in size and became undetectable 18–23 days after treatment with either CD28 ζ or 41BB ζ B7-H3.CAR-T cells (figure 3A,E,I). CAR-T cell treatment improved the survival of the mice (online supplemental figure S4B,F,J), with mice still tumor-free when the experiments were terminated 92, 84, and 95 days post WHIM12, WHIM2 and WHIM30 injection, respectively. Peripheral blood and bone marrow were analyzed at the time of euthanasia. Both CD28 ζ and 41BB ζ B7-H3.CAR-T cells were detectable (figure 3B,F,J), and exhibited similar composition in effector and memory cell subsets within each PDX model (figure 3C,G,K), and similar exhausted cells identified by coexpression of PD-1 and TIM3 (figure 3D,H,L). Similar distribution of memory and exhausted cell subsets was observed for CD28 ζ and 41BB ζ B7-H3.CAR-T cells collected from the bone marrow (online supplemental figure S4C–E, G–I, K–M). Finally, we performed experiments in which mice engrafted with the most aggressive PDX line WHIM12 were treated with a lower dose (2.5×10^6) of B7-H3.CAR-T cells. In this stress model, B7-H3.CAR-T cells encoding CD28 showed the most prominent capacity to control the tumor growth (figure 3M). As in the other PDX TNBC tumor models, we did not observe significant differences in the numbers and cell subset compositions of circulating CD28 ζ and 41BB ζ B7-H3.CAR-T cells (figure 3N,O). However, B7-H3.CAR-T cells encoding CD28 showed a reduced percentage of T cells coexpressing PD-1 and TIM3 (figure 3P). Overall, these data support the antitumor activity of the B7-H3.CAR-T cells against PDX

TNBC cells in vivo and the superiority conferred by the CD28 costimulation under stress conditions.

CSPG4 is a critical B7-H3 complementary target for TNBC

Although B7-H3 protein is highly expressed in TNBC, 40 of the 159 (25%) cores analyzed showed dim B7-H3 protein expression, with H-score at or below the lower quartile threshold (≤ 105) (online supplemental figure S5A–D), which may favor tumor escape. Here, we analyzed the same samples from the AURORA US Network cohort and UNC Rapid Autopsy Program cohort³⁰ for the expression of the *CSPG4* gene. First, we assessed the expression of *CSPG4* in 98 TNBC samples, and observed that *CSPG4* mRNA was broadly detected in both primary and metastatic tumors (figure 4A). When all BC tumors were included, the study showed overall preserved *CSPG4* mRNA expression between primary and metastatic lesions (figure 4B). Further stratification by the most common sites of metastasis showed no significant differences, except for luminal liver metastases compared with primary breast tumors (figure 4C). When tumors were grouped by intrinsic molecular subtypes and site of metastasis, *CSPG4* mRNA expression in the luminal group showed a significant reduction in liver metastases compared with their primary counterparts ($p = 3.3 \times 10^{-9}$). Similarly to *CD276*, *CSPG4* mRNA levels were generally maintained between primary tumors and metastases when analyzing all subtypes or BL tumors, but were significantly lower in metastatic tumors within the luminal-HER2E group (online supplemental figure S5E–I). We further analyzed the RNA sequencing (RNA-seq) dataset to assess the concurrent expression of *CD276* and *CSPG4* mRNA in 96 TNBC samples, both primary and metastatic. Tumors were classified based on gene expression thresholds at the 25th percentile (figure 4D–G). Notably, tumors with simultaneous high expression of both *CSPG4* and *CD276* genes above the 25th percentile, referred to as “High-High,” accounted for 68% of primary tumors and 66% of metastatic lesions (figure 4E). Importantly, none of the tumors in the combined dataset exhibited concurrent low expression of both *CSPG4* and *CD276* genes, categorized as “Low-Low” (figure 4E). Furthermore, in 100% of cases, either *CSPG4* or *CD276* genes demonstrated high expression (figure 4F). Baseline expression analysis of TNBC in primary and metastatic tumors revealed that *CSPG4* and *CD276* genes are frequently coexpressed, with no gene expression levels falling below a value of 6 (figure 4G). Specifically, when one gene displayed lower expression levels, the other remained highly expressed (figure 4G). We then evaluated *CSPG4* protein expression by immunohistochemistry in 151 available TNBC cores, in which B7-H3 expression was assessed. The median *CSPG4* H-score was 33, with lower and upper quartiles of 14 and 78, respectively (figure 5A,B). Notably, at least 18 out of 37 cores (49%) with B7-H3 H-score ≤ 105 (lower quartile) exhibited a *CSPG4* H-score exceeding its median value (figure 5C,D). Furthermore, among cores with low B7-H3 expression (H-score between the lower quartile, >105 ,

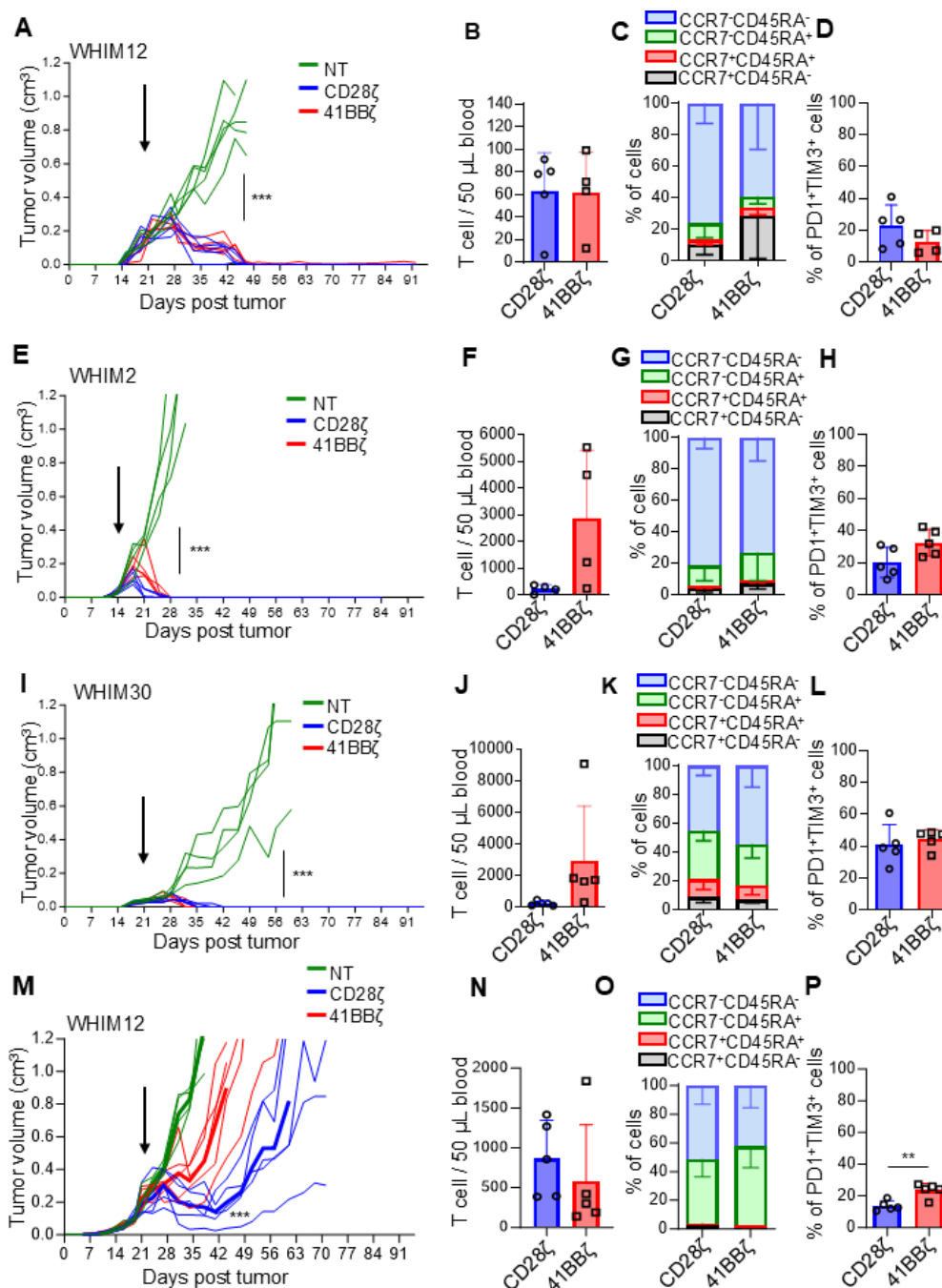


Figure 3 CD28 costimulation provides superior antitumor effects of B7-H3.CAR-T cells in PDX TNBC models under stress conditions. (A, E, I) Tumor growth in NSG mice engrafted with the PDX WHIM12 (A), WHIM2 (E) or WHIM30 (I) in the right mammary fat pad, and treated with control non-transduced T cells (NT) or B7-H3.CAR-T cells encoding either CD28 ζ or 41BB ζ by intravenous injection (5×10^6 CAR-T cells). Mice were treated at day 21 (WHIM12 and WHIM30 models) or day 14 (WHIM2 model) after tumor implant. Arrows indicate the time of T-cell treatment. Tumors were measured two times a week with a digital caliper; $n=4-5$ mice per group, *** $p<0.0001$ (day 47 in A; day 32 in E), *** $p=0.0006$ (day 60 in I) by one-way ANOVA followed by unpaired Student's t-test for group comparison. (B, F, J) Quantification of the CAR-T cells in the peripheral blood of the WHIM12 (B), WHIM2 (F) and WHIM30 (J) PDX models. (C, G, K) Phenotypic characterization of circulating CAR-T cells based on the expression of CCR7 and CD45RA in the WHIM12 (C), WHIM2 (G) and WHIM30 (K) PDX models. (D, H, L) Coexpression of PD-1 and TIM3 in circulating CAR-T cells in the WHIM12 (D), WHIM2 (H) and WHIM30 (L) PDX models; $n=4-5$ mice per group, data are shown as mean \pm SD. (M) Tumor growth in mice engrafted with the PDX WHIM12 in the right mammary fat pad and treated with control NT T cells or B7-H3.CAR-T cells encoding either CD28 ζ or 41BB ζ by intravenous injection (2.5×10^6 CAR-T cells) on day 17; $n=5$ mice per group, *** $p=0.0007$ at day 44 by one-way ANOVA followed by unpaired Student's t-test for group comparison. (N-P) Quantification of the CAR-T cells in the peripheral blood (N), and their phenotypic characterization based on the expression of CCR7 and CD45RA (O) and the coexpression of PD-1 and TIM3 (P); $n=5$ mice per group, data are shown as mean \pm SD, ** $p=0.004$ by unpaired Student's t-test. ANOVA, analysis of variance; CAR, chimeric antigen receptor; TNBC, triple-negative breast cancer.

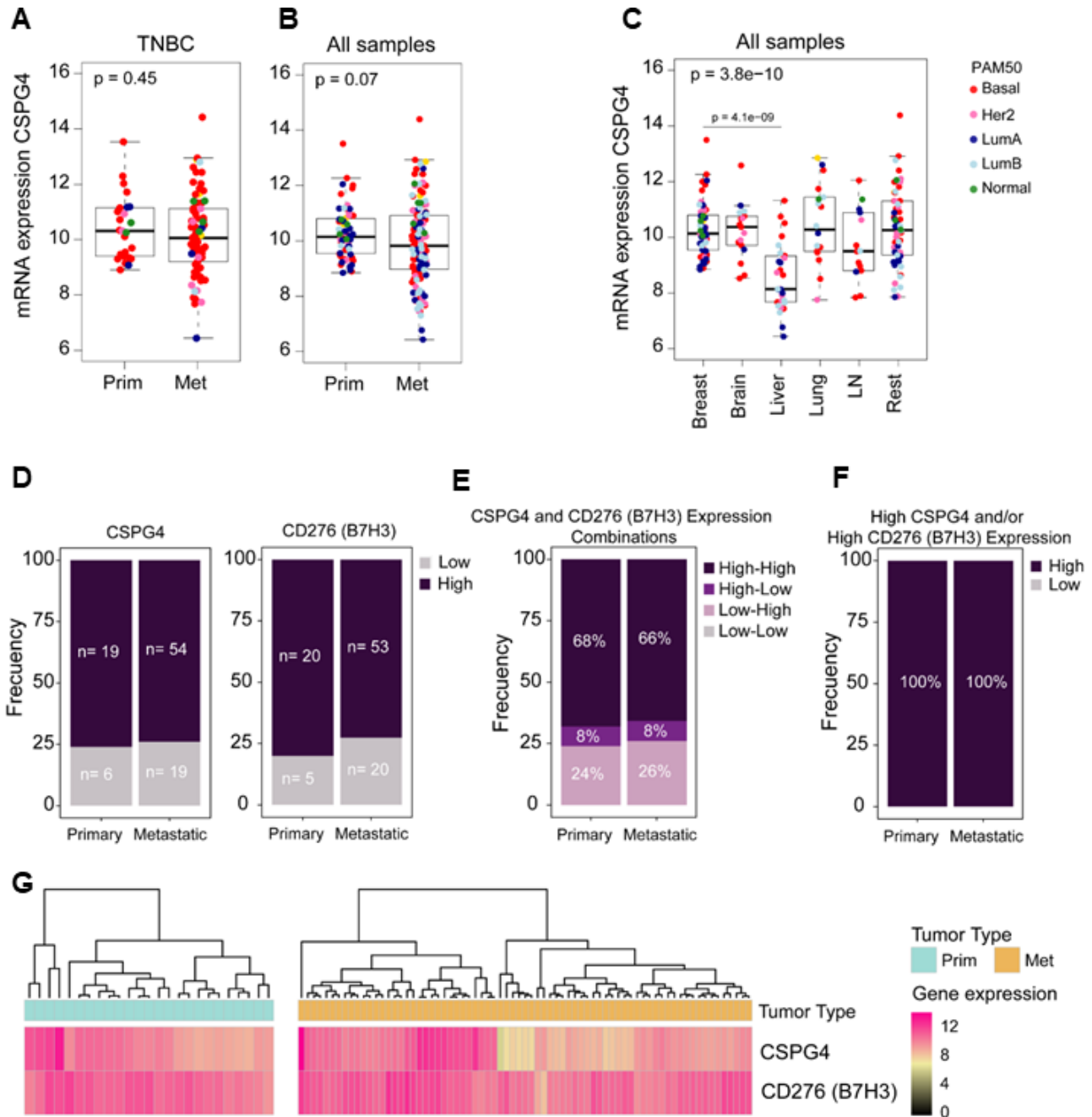


Figure 4 Comparative expression of *CSPG4* and *CD276* genes in TNBC. (A) Expression of *CSPG4* mRNA in 98 TNBC samples of a combined set of 205 BC samples, consisting of 64 primary tumors and 141 metastatic lesions. (B) Expression of *CSPG4* mRNA across all samples (primaries and metastases combined) (TNBC=98, ER⁺/HER2⁻=76, HER2⁺=34). (C) *CSPG4* mRNA expression across all samples, stratified by the most common metastatic sites. All box and whisker plots of the figure display the median value on each bar, showing the data's lower and upper quartile range (Q1–Q3). The whiskers represent the lines from the minimum value to Q1 and Q3 to the maximum value. All comparisons between more than two groups were performed by analysis of variance with a post hoc Tukey test (one-sided). The p values for the post hoc test are shown. A comparison between only two groups was performed using an unpaired t-test (two-sided). mRNA expression is shown as a relative expression of log2-transformed batch-corrected data. (D) Bar plots illustrating the incidence of tumors with high and low gene expression levels of *CSPG4* and *CD276* in primary and metastatic TNBC samples. Dark purple bars represent the high group (tumors with gene expression values above the 25th percentile) and light purple bars represent the low group (tumors with gene expression values below the 25th percentile). (E) Bar plots showing the frequency of tumors grouped by the combined expression levels of *CSPG4* and *CD276* genes, categorized into four groups: High-High, High-Low, Low-High, and Low-Low, divided by primary and metastatic tumors. (F) Bar plots illustrating the frequency of tumors that exhibit high expression of *CSPG4* and/or *CD276* genes, divided by primary and metastatic tumors. (G) Heatmap displaying the gene expression values of *CSPG4* and *CD276* genes, divided by primary and metastatic tumors. *CSPG4*, chondroitin sulfate proteoglycan 4; LN, lymph node; LumA, luminal A; LumB, luminal B; Met, metastatic tumor; mRNA, messenger RNA; normal, normal-like; Prim, primary tumor; Rest, other sites of metastasis; TNBC, triple-negative breast cancer.

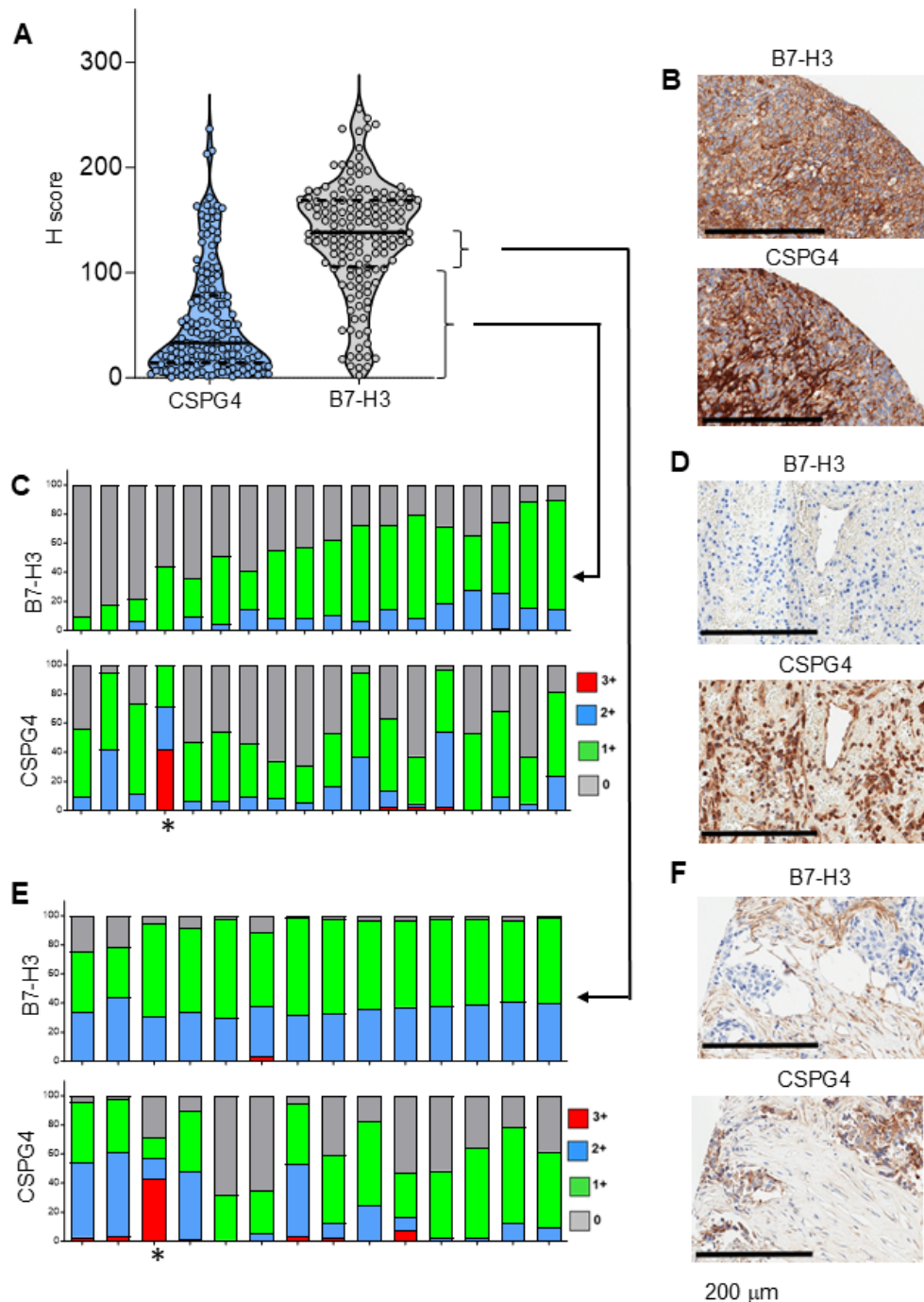


Figure 5 B7-H3 and CSPG4 protein expression in TNBC. (A) Violin plots showing B7-H3 and CSPG4 H-score of 151 TNBC cores evaluable for the analyses of both antigens. Solid lines indicate the median and the dotted lines indicate the lower and upper quartiles. (B) Representative immunohistochemistry of a TNBC core analyzed for B7-H3 and for CSPG4 expression (high expression). Bars represent 200 µm (magnification 20×; images captured using Aperio ImageScope). (C) Visualization of B7-H3 and CSPG4 expression in 18 TNBC cores. These representative cores are selected from 37 TNBC cores in which B7-H3 H-score is in the lower quartile (≤ 105) and the CSPG4 H-score exceeds its median value (> 33). Each stacked bar represents a core of TNBC and in each segment, the frequency of cells in each core with high (3+), moderate (2+), low (+1), and negative (0) expressions for B7-H3 and CSPG4. (D) Representative imaging of a TNBC core analyzed for B7-H3 and CSPG4 expression in the samples described in (C); the bars represent 200 µm (magnification 20×; images were captured using Aperio ImageScope). *Indicates the core for which images are shown. (E) Visualization of B7-H3 and CSPG4 expression in 14 cores of TNBC. These representative cores are selected from the 37 TNBC cores in which B7-H3 H-score ranges between the lower quartile (> 105) and the median (≤ 138), and the CSPG4 H-score exceeds its median value (> 33). Each stacked bar represents a core of TNBC. Each segment represents the frequency of cells in each core expressing high (3+), moderate (2+), low (+1), and negative (0) expression for B7-H3 and CSPG4. (F) Representative imaging of a TNBC core analyzed for B7-H3 and CSPG4 expression in the sample described in (E); bars represent 200 µm (magnification 20×; images captured using Aperio ImageScope). *Indicates the core for which images are shown. CSPG4, chondroitin sulfate proteoglycan 4; TNBC, triple-negative breast cancer.

and median, ≤ 138), 14 out of 37 cores (38%) scored CSPG4 expression above its median H-Score, while seven samples (18%) had CSPG4 expression exceeding its upper quartile (figure 5E,F). Only 9 out of 151 TNBC cores (6%) showed B7-H3 and CSPG4 expression below their respective lower quartile. CSPG4 protein expression was also evaluated by immunohistochemistry in the available cohort of 614 BC samples analyzed for the B7-H3 expression. The median H-score for CSPG4 expression in all non-TNBC BC samples was relatively lower compared with B7-H3, with a median value of 52 and lower and upper quartile of 23 and 97, respectively (online supplemental figure S5J). As previously reported,^{27,28} CSPG4 was not expressed in normal breast tissues (online supplemental figure S5K). Overall, these data support the potential clinical relevance of dual targeting of B7-H3 and CSPG4 in TNBC to prevent tumor escape as the majority of tumors express one or both proteins.

Dual CAR-T cells co-targeting B7-H3 and CSPG4 with optimized in trans costimulation eradicate tumors with mixed antigen expression

We constructed dual CAR-T cells targeting both CSPG4 and B7-H3 by combining either the B7-H3.CAR encoding CD28 and CD3 ζ with the CSPG4.CAR incorporating the 4-1BB endodomain (DCAR1), or the CSPG4.CAR encoding CD28 and CD3 ζ with the B7-H3.CAR featuring the 4-1BB endodomain (DCAR2)¹⁴ (figure 6A). Both dual CAR cassettes were successfully expressed in human T cells (figure 6B) without alteration in their phenotypic composition (online supplemental figure S6B,C). To study the specificity of each component of the dual CAR cassettes, we used the TNBC PDX line WHIM12 (WT) that physiologically expresses both B7-H3 and CSPG4 (online supplemental figure S3A,B and S6D), and generated clones of these cells in which we ablated either the *CD276* gene (B7-H3^{KO}) or the *CSPG4* (CSPG4^{KO}) gene using the CRISPR/Cas9 technology (figure 6C). We co-cultured CSPG4^{KO} and B7-H3^{KO} cells with either CSPG4.CAR-T cells, B7-H3.CAR-T cells or the dual CAR (DCAR1 and DCAR2) T cells at a low E:T ratio (1:5). CSPG4.CAR, B7-H3.CAR, DCAR1 and DCAR2 T cells eliminated the WT cell line, while CSPG4.CAR and B7-H3.CAR T cells failed to eliminate CSPG4^{KO} and B7-H3^{KO} cells, respectively. Remarkably, DCAR2 T cells efficiently eliminated both CSPG4^{KO} and B7-H3^{KO} cells, while DCAR1 T cells efficiently eliminated CSPG4^{KO} cells, but were unable to remove completely the B7-H3^{KO} cells (figure 6D and online supplemental figure S4E). The observed difference in antitumor activity between DCAR1 and DCAR2 T cells was reflected by differences in the CAR-T cell cytokine release in the co-culture experiments, as DCAR2 T cells released IFN- γ in response to both CSPG4^{KO} and B7-H3^{KO} tumor cells, while DCAR1 T cells did not release IFN- γ in the presence of B7-H3^{KO} tumor cells (figure 6E). Similar results were obtained for IL-2 release and CAR-T cell proliferation when DCAR1 and DCAR2 T cells were co-cultured with CSPG4^{KO} or B7-H3^{KO} tumor cells (online

supplemental figure S4F,G). To explain the superior mode of action of DCAR2 T cells in vitro, we measured T-cell activation based on CD69 expression when control NT T cells, DCAR1 and DCAR2 T cells were stimulated with either B7-H3^{KO} or CSPG4^{KO} tumor cells. We found that DCAR2 T cells displayed high activation in response to both B7-H3^{KO} and CSPG4^{KO} tumor cells, while DCAR1 T cells were suboptimally activated in response to B7-H3^{KO} tumor cells (figure 6F). We then quantified the density of B7-H3 and CSPG4 antigens on tumor cells by flow cytometry and observed that B7-H3 antigen density is higher than CSPG4 antigen density in WHIM12 cells (figure 6G). We orthotopically engrafted NSG mice with a mixture (1:1 ratio) of B7-H3^{KO} and CSPG4^{KO} tumor cells and treated them with low dose (2.5×10^6) of either CSPG4.CAR, B7-H3.CAR, DCAR1 or DCAR2 T cells 18 days later. Recapitulating the results of the in vitro experiments, T cells expressing the DCAR2 demonstrated superior tumor control (figure 7A,B). Immunohistochemistry of the tumors confirmed the specificity of CAR-T cell targeting in vivo. Specifically, mice treated with control NT T cells showed growth of tumors expressing CSPG4 and B7-H3. Mice treated with B7-H3.CAR-T cells showed growth of tumors expressing CSPG4 alone, while mice treated with CSPG4.CAR-T cells showed growth of tumors expressing B7-H3 alone (figure 7C). Mice treated with DCAR1 T cells showed growth of tumors expressing CSPG4, confirming the in vitro data that CAR-T cells targeting CSPG4 with in trans expression of 4-1BB without CD3 ζ cannot efficiently eliminate tumor cells with low density of the targeted antigen (figure 7C). We monitored the T cells in the peripheral blood of treated mice, and DCAR2 T cells were more abundant at day 21 after treatment than B7-H3.CAR, CSPG4.CAR or DCAR1 T cells (figure 7D). There were no significant changes in CAR-T cell phenotypic composition based on the expression of CD45 and CCR7, but DCAR2 T cells showed reduced cells coexpressing TIM3 and PD-1, indicative of an exhausted phenotype (figure 7E,F). Overall, these data indicate that the optimal design of the B7-H3 and CSPG4 CAR co-targeting allows the eradication of TNBC with mixed antigen expression.

DISCUSSION

The identification of the most appropriate antigens and antigen combinations to be targeted with CAR-T cells in solid tumors including TNBC remains a high priority to ensure safety and prevent tumor escape. Here we report a comprehensive analysis of the expression of B7-H3 and CSPG4 in TNBC. Our results highlight that none of the primary and metastatic TNBC analyzed lack the expression of the two genes simultaneously, and that 94% of the 151 cores of TNBC analyzed showed expression of at least one of these two proteins, with only 6% of the cores showing both proteins simultaneously below their respective lower quartile H-score. We further demonstrated that co-targeting B7-H3 and CSPG4 with bispecific CAR-T cells

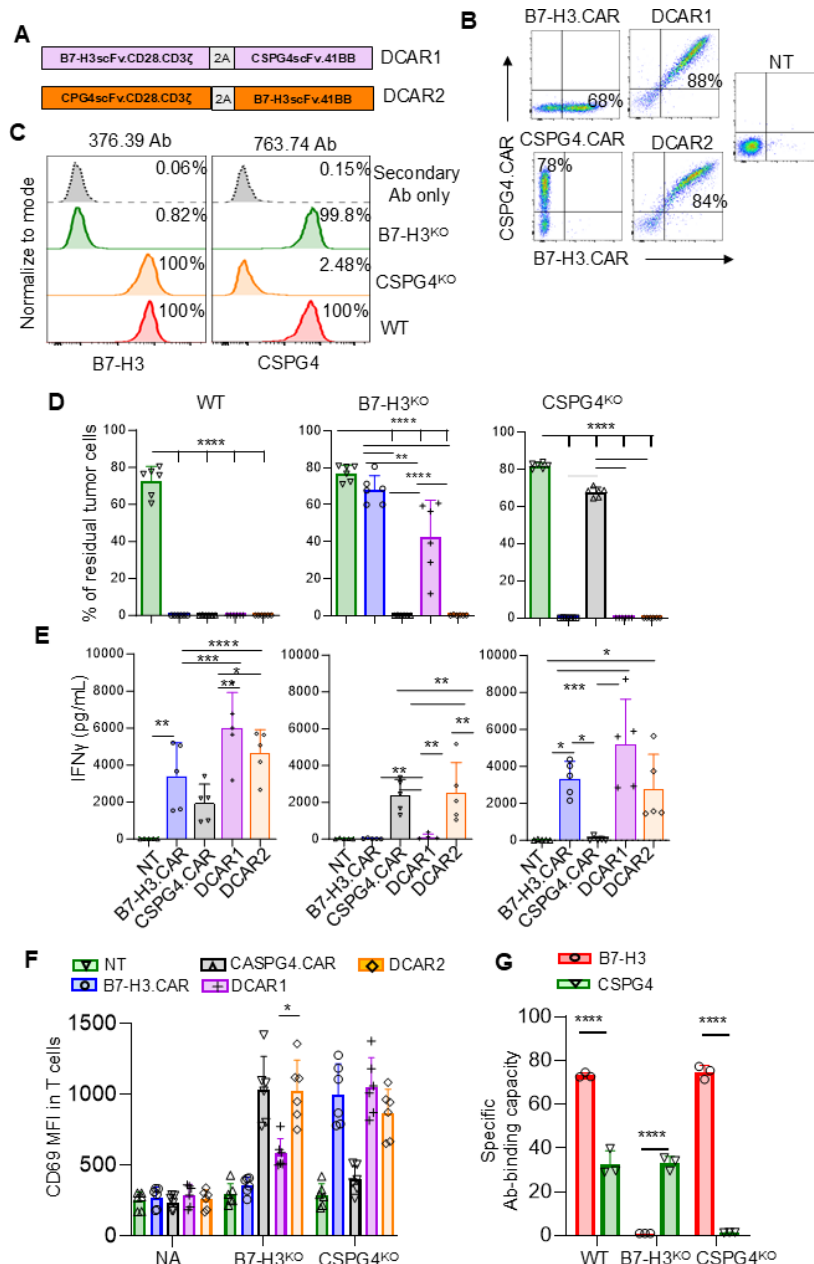


Figure 6 Antigen density is critical for efficient trans CAR-T cell costimulation of B7-H3 and CSPG4 dual targeting. (A) Schematic representation of retroviral vectors encoding the dual B7-H3 and CSPG4 CARs with split CD28 and 4-1BB costimulation and shared CD3ζ chain. (B) Representative flow cytometry plots showing B7-H3.CAR and CSPG4.CAR expression in T cells transduced with B7-H3.CAR, CSPG4.CAR, or the dual specific CARs, DCAR1 or DCAR2. NT indicates control non-transduced T cells. (C) Histograms showing the expression of B7-H3 and CSPG4 in WHIM12 WT cells (WT), B7-H3^{KO}CSPG4⁺ (B7-H3^{KO}) WHIM12 cells and B7-H3⁺CSPG4^{KO} (CSPG4^{KO}) WHIM12 cells, using either the 376.96 Ab or the 763.74 Ab used to generate the B7-H3.CAR and CSPG4.CAR, respectively. The secondary Ab alone was used as a negative control for the staining. (D, E) Control non-transduced T cells (NT), B7-H3.CAR, CSPG4.CAR, DCAR1 and DCAR2 T cells were co-cultured with WT, B7-H3^{KO} or CSPG4^{KO} cells at a 1:5 effector to target ratio. At day 5, cells were collected, and tumor cells and T cells were enumerated by flow cytometry. Data illustrate the summary of residual tumor cells at day 5 of culture (D) and IFN-γ (E) detected in the culture supernatant collected at 24 hours by ELISA; n=5–6, data are shown as mean±SD, ****p<0.0001, **p=0.0032, *p=0.0011 by one-way ANOVA with Tukey's correction (D) and ****p<0.0001, ***p=0.0003, **p=0.007, *p=0.039 by one-way ANOVA with Tukey's correction (E). (F) Control NT T cells, B7-H3.CAR, CSPG4.CAR, DCAR1, and DCAR2 T cells were stimulated with either B7-H3^{KO} or CSPG4^{KO} cells for 6 hours, and then CD69 MFI was assessed by flow cytometry in T cells as a marker of activation. Non-stimulated T cells served as negative control; n=6, data are shown with mean±SD, *p=0.0255 (DCAR1 vs DCAR1 B7-H3^{KO}) by two-way ANOVA with Tukey's correction. (G) Quantification of the antigen density in WT, B7-H3^{KO} and CSPG4^{KO} WHIM12 cells, calculated as specific antibody binding capacity for both the B7-H3 and CSPG4 antigens; n=3, data are shown with mean±SD, ****p<0.0001 by one-way ANOVA with Tukey's correction. Abs, antibodies; ANOVA, analysis of variance; CAR, chimeric antigen receptor; CSPG4, chondroitin sulfate proteoglycan 4; IFN, interferon; MFI, mean fluorescence intensity; scFv, single chain variable fragment.

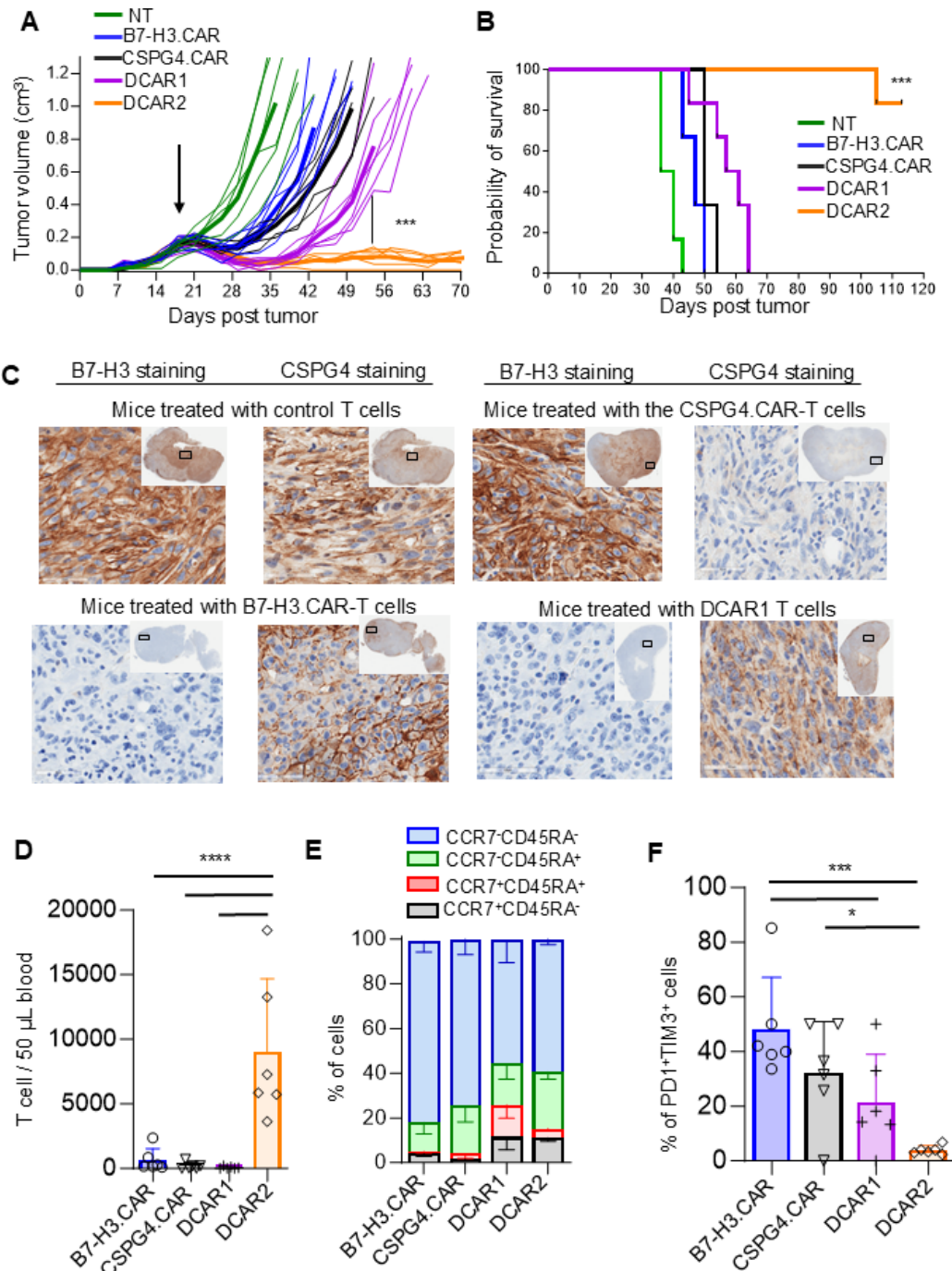


Figure 7 B7-H3 and CSPG4 dual targeting eliminates TNBC PDX with mixed antigen expression in vivo. (A) Tumor growth in mice engrafted with WHIM12 B7-H3^{KO}CSPG4⁺ (B7-H3^{KO}) tumor cells mixed with WHIM12 B7-H3⁺CSPG4^{KO} (CSPG4^{KO}) cells at a 1:1 ratio in the right mammary fat pad and treated with either control non-transduced T cells (NT), B7-H3.CAR, CSPG4.CAR, DCAR1, and DCAR2 T cells (2.5×10^6 T cells) by intravenous injection at day 18 after tumor implantation. The arrow indicates the time of T-cell treatment. Tumors were measured twice a week with a digital caliper; $n=6$ mice per group, *** $p=0.0002$ at day 35 by one-way ANOVA followed by unpaired Student's t-test for group comparison. Data are representative of one of two independent experiments. (B) Kaplan-Meier survival curve of mice shown in (A); *** $p<0.0001$. (C) Representative immunohistochemistry images of B7-H3 and CSPG4 expressions in tumors growing in mice described in (A) at the time of euthanasia. Bars represent 60 μ m (magnification 40 \times ; images captured using Aperio ImageScope). (D) T-cell counts in the peripheral blood of mice described in (A) at day 21 after CAR-T cell treatment; $n=6$ mice per group, data are shown as mean \pm SD, *** $p=0.0003$ (B7-H3 vs CAR2), *** $p=0.002$ (B7-H3 vs CAR2), *** $p=0.001$ (DCAR1 vs DCAR2), by one-way ANOVA with Tukey's correction. (E, F) Phenotypic characterization of circulating CAR-T cells in the model described in (A) based on the expression of CCR7 and CD45RA (E) and the coexpression of PD-1 and TIM3 (F); $n=6$, data are shown as mean \pm SD, *** $p=0.00051$, * $p=0.0275$ (CSPG4.CAR vs DCAR2), * $p=0.0387$ (B7-H3.CAR vs DCAR1) by one-way ANOVA with Tukey's correction. ANOVA, analysis of variance; CAR, chimeric antigen receptor; CSPG4, chondroitin sulfate proteoglycan 4; PDX, patient derived xenograft; PD-1, programmed cell death protein 1; TNBC, triple-negative breast cancer.

would allow the development of a CAR cassette applicable to the great majority of patients with TNBC and prevent tumor escape.

Systematic analyses of the expression of antigens that can be co-targeted with CAR-T cells in a large cohort of TNBC samples are lacking. Our analysis of *CD276* mRNA expression in 98 TNBC samples indicates that B7-H3 is overexpressed and is maintained in different anatomic locations of tumor metastases. Furthermore, immunohistochemistry analysis of 159 TNBC cores, confirmed medium-high expression of B7-H3 in 77% of the cases. Of note, B7-H3 expression was also conserved in other types of BC. Encouraged by these analyses, we assessed the functionality of the B7-H3.CAR-T cells in three representative TNBC PDX models confirming their potent anti-tumor activity. In the most aggressive TNBC PDX model, we observed that CD28 costimulation provides the most effective antitumor activity when low doses of CAR-T cells were used. This likely reflects the rapid mode of activation of CD28 costimulated CAR-T cells that we and others have previously reported when comparing CD28 and 4-1BB costimulation in CAR-T cells.^{40 41} Based on these results, we have initiated a Phase I clinical study to test the safety and antitumor activity of autologous B7-H3.CAR-T cells encoding the CD28 endodomain and coexpressing the iC9 safety switch in patients with relapsed/refractory TNBC (NCT06347068).

Our characterization of B7-H3 expression in TNBC samples by immunohistochemistry shows that 40 of the 159 analyzed cores (25%) display dim B7-H3 expression (below the lower quartile, H-score ≤ 105), which may favor tumor escape. To develop a strategy to target simultaneously two antigens and prevent tumor escape due to heterogeneous antigen expression, we analyzed the expression patterns of *CSPG4* in TNBC. In our dataset of 98 TNBC samples, we observed that *CSPG4* gene expression closely matches the trend of *CD276* gene expression. Importantly, none of the tumors in the combined dataset exhibited concurrent low expression of both *CSPG4* and *CD276* genes. Immunohistochemistry analysis of 151 available TNBC cores for which we had tested the expression of B7-H3 revealed that the H-score for *CSPG4* expression was overall lower than B7-H3. However, 94% of the core with low B7-H3 H-scores exhibited targetable levels of *CSPG4* expression, indicating that co-targeting B7-H3 and *CSPG4* could enable the development of a CAR-T cell product with potential clinical activity in the great majority of patients with TNBC. We were unable to compare mRNA and protein expression of B7-H3 and *CSPG4* in the same samples. However, the public CPTAC BC data set in which RNA-seq and mass spec proteomics for ~8,000 genes have been analyzed⁴² shows that the correlation for *CSPG4* protein versus mRNA is 0.786, and for B7-H3/*CD276* is 0.54, suggesting that the detection of protein expression remains fundamental for the identification of targetable antigens by CAR-T cells. The potential for clinical translation of our proposed dual B7-H3 and *CSPG4* co-targeting strategy is supported by our ongoing

Phase I clinical trial (NCT06096038), in which patients with head and neck cancer are treated with autologous *CSPG4*.CAR-T cells encoding CD28 and coexpressing the iC9 safety switch. Safety data from this trial will help inform future application in TNBC.

Bispecific CAR-T cells with tandem CAR design have been explored in lymphoid malignancies with modest clinical activity.^{12 13} We previously reported the development of a bispecific CAR design that provides transacting CD28 and 4-1BB costimulation, and forms a unique CAR synapse ensuring appropriate T-cell costimulation and metabolic fitness.¹⁴ The proposed bispecific CAR design with a shared CD3 ζ chain attenuates the CD3 ζ chain signaling when two CARs are simultaneously activated,¹⁴ and is in line with the observation that attenuating the CD3 ζ signaling, by reducing the number of tyrosine residues within the CD3 ζ chain that can be phosphorylated, reduces the activation of CAR-T cells and potentially lessens their toxicity.^{43 44} The concept of dual targeting with split costimulation and shared CD3 ζ chain signaling has been adapted by other investigators, underlining the flexibility and reproducibility of the proposed design.^{44 45} Here we show that CAR-T cells co-targeting B7-H3 and *CSPG4* represent a valuable therapeutic strategy for TNBC. In a clinically relevant PDX tumor model with heterogeneous intratumor antigen expression, bispecific CAR-T cells targeting simultaneously B7-H3 and *CSPG4* eradicated the tumor. Our data also underlines the critical observation that the optimal design of a bispecific CAR is strictly associated with the density of the targeted antigens. Both antigen density and affinity of the CAR binder for the antigen are key factors in determining CAR-T cell activity, on-target off-tumor toxicity and potential tumor escape.^{9 10 18 46 47} Here we highlight that B7-H3 is expressed at a higher density in TNBC compared with *CSPG4*, and that for effective dual targeting using the split costimulation design, the optimal 4-1BB signaling is achieved when the CAR targets the high-density antigen (B7-H3), while CD28 and CD3 ζ signaling are sufficiently activated by the low-density antigen (*CSPG4*).

In summary, we present clinically relevant evidence that co-targeting B7-H3 and *CSPG4* with an optimized dual CAR can enable the generation of a single CAR cassette that can be used to treat the great majority of patients with TNBC because at least one of these antigens is expressed by tumor cells. Furthermore, co-targeting B7-H3 and *CSPG4* could benefit a broader population of patients with BC, as we observed a similar pattern of B7-H3 and *CSPG4* expression across other BC subtypes as seen in TNBC.

Author affiliations

¹Lineberger Cancer Center, University of North Carolina, Chapel Hill, North Carolina, USA

²Department of Genetics, University of North Carolina at Chapel Hill, Chapel Hill, North Carolina, USA

³Pathology & Laboratory Medicine, University of North Carolina at Chapel Hill, Chapel Hill, North Carolina, USA

⁴Division of Oncology, University of North Carolina at Chapel Hill, Chapel Hill, North Carolina, USA

⁵Department of Pediatrics, University of North Carolina, Chapel Hill, North Carolina, USA

⁶Department of Microbiology and Immunology, University of North Carolina, Chapel Hill, North Carolina, USA

Contributors SS designed and performed the majority of experiments, analyzed data and wrote the manuscript. RB, MZ, EC, CMP and PDR assisted with experiments. SG-R and CMP performed and wrote the bioinformatics analysis. SO and LC provided the tumor samples and analyzed the immunohistochemistry data. HSE, CMP and LC provided critical clinical knowledge. GD and BS conceived of, oversaw and directed the research, obtained research funding and wrote the manuscript. All authors reviewed and approved the manuscript. Guarantor information: GD is the guarantor of the overall content of the manuscript and accepts full responsibility for the finished work and conduct of the study. GD has access to the data and controlled the decision to publish.

Funding This work was supported in part by P50-CA058233 (CP, GD) from the National Cancer Institute and UNC Lineberger Center for Triple Negative Breast Cancer. The UNC Small Animal Imaging Facility at the Biomedical Imaging Research Center, the Pathology Service Core, the Laboratory Medicine, and the Flow Cytometry Core Facilities are supported in part by an NCI Cancer Center Core Support Grant to the UNC Lineberger Comprehensive Cancer Center (P30-CA016086-40), the AURORA and Rapid Autopsy Programs are supported by the Breast Cancer Research Foundation and Susan G Komen (LC, CMP).

Competing interests GD serves in the SAB of NanoCells, Estella, Arovela and Outspace Bio. GD is cofounder of Persistence Bio. A patent application for the dual CAR has been filed. CMP is an equity stockholder and consultant of BioClassifier LLC; CMP is also listed as an inventor on patent applications for the Breast PAM50 subtyping assay.

Patient consent for publication Not applicable.

Ethics approval Six TMAs were constructed by the UNC-TPL under UNC protocol LCCC9830, using tumor tissues collected from patients with BC being seen and consented at UNC Hospital. Immunohistochemistry was performed by the UNC-TPL (under IRB protocol TMA-1930, #21-0792).

Provenance and peer review Not commissioned; externally peer reviewed.

Data availability statement Data are available upon reasonable request.

Supplemental material This content has been supplied by the author(s). It has not been vetted by BMJ Publishing Group Limited (BMJ) and may not have been peer-reviewed. Any opinions or recommendations discussed are solely those of the author(s) and are not endorsed by BMJ. BMJ disclaims all liability and responsibility arising from any reliance placed on the content. Where the content includes any translated material, BMJ does not warrant the accuracy and reliability of the translations (including but not limited to local regulations, clinical guidelines, terminology, drug names and drug dosages), and is not responsible for any error and/or omissions arising from translation and adaptation or otherwise.

Open access This is an open access article distributed in accordance with the Creative Commons Attribution Non Commercial (CC BY-NC 4.0) license, which permits others to distribute, remix, adapt, build upon this work non-commercially, and license their derivative works on different terms, provided the original work is properly cited, appropriate credit is given, any changes made indicated, and the use is non-commercial. See <http://creativecommons.org/licenses/by-nc/4.0/>.

ORCID iD

Gianpietro Dotti <http://orcid.org/0000-0002-2639-8526>

REFERENCES

- Perou CM, Sorlie T, Eisen MB, et al. Molecular portraits of human breast tumours. *Nature New Biol* 2000;406:747–52.
- Prat A, Ellis MJ, Perou CM. Practical implications of gene-expression-based assays for breast oncologists. *Nat Rev Clin Oncol* 2011;9:48–57.
- Perou CM, Parker JS, Prat A, et al. Clinical implementation of the intrinsic subtypes of breast cancer. *Lancet Oncol* 2010;11:718–9.
- Prat A, Adamo B, Cheang MCU, et al. Molecular characterization of basal-like and non-basal-like triple-negative breast cancer. *Oncologist* 2013;18:123–33.
- Schmid P, Salgado R, Park YH, et al. Pembrolizumab plus chemotherapy as neoadjuvant treatment of high-risk, early-stage triple-negative breast cancer: results from the phase 1b open-label, multicohort KEYNOTE-173 study. *Ann Oncol* 2020;31:569–81.
- Schmid P, Cortes J, Pusztai L, et al. Pembrolizumab for Early Triple-Negative Breast Cancer. *N Engl J Med* 2020;382:810–21.
- Tchou J, Zhao Y, Levine BL, et al. Safety and Efficacy of Intratumoral Injections of Chimeric Antigen Receptor (CAR) T Cells in Metastatic Breast Cancer. *Cancer Immunol Res* 2017;5:1152–61.
- Srivastava S, Furlan SN, Jaeger-Ruckstuhl CA, et al. Immunogenic Chemotherapy Enhances Recruitment of CAR-T Cells to Lung Tumors and Improves Antitumor Efficacy when Combined with Checkpoint Blockade. *Cancer Cell* 2021;39:193–208.
- Caruso HG, Hurton LV, Najjar A, et al. Tuning Sensitivity of CAR to EGFR Density Limits Recognition of Normal Tissue While Maintaining Potent Antitumor Activity. *Cancer Res* 2015;75:3505–18.
- Walker AJ, Majzner RG, Zhang L, et al. Tumor Antigen and Receptor Densities Regulate Efficacy of a Chimeric Antigen Receptor Targeting Anaplastic Lymphoma Kinase. *Mol Ther* 2017;25:2189–201.
- O'Rourke DM, Nasrallah MP, Desai A, et al. A single dose of peripherally infused EGFRvIII-directed CAR T cells mediates antigen loss and induces adaptive resistance in patients with recurrent glioblastoma. *Sci Transl Med* 2017;9:eaaa0984.
- Grada Z, Hegde M, Byrd T, et al. TanCAR: A Novel Bispecific Chimeric Antigen Receptor for Cancer Immunotherapy. *Mol Ther Nucleic Acids* 2013;2:e105.
- Spiegel JY, Patel S, Muffly L, et al. CAR T cells with dual targeting of CD19 and CD22 in adult patients with recurrent or refractory B cell malignancies: a phase 1 trial. *Nat Med* 2021;27:1419–31.
- Hirabayashi K, Du H, Xu Y, et al. Dual Targeting CAR-T Cells with Optimal Costimulation and Metabolic Fitness enhance Antitumor Activity and Prevent Escape in Solid Tumors. *Nat Cancer* 2021;2:904–18.
- Chapoval AI, Ni J, Lau JS, et al. B7-H3: a costimulatory molecule for T cell activation and IFN-gamma production. *Nat Immunol* 2001;2:269–74.
- Picarda E, Ohaegbulam KC, Zang X. Molecular Pathways: Targeting B7-H3 (CD276) for Human Cancer Immunotherapy. *Clin Cancer Res* 2016;22:3425–31.
- Yamato I, Sho M, Nomi T, et al. Clinical importance of B7-H3 expression in human pancreatic cancer. *Br J Cancer* 2009;101:1709–16.
- Du H, Hirabayashi K, Ahn S, et al. Antitumor Responses in the Absence of Toxicity in Solid Tumors by Targeting B7-H3 via Chimeric Antigen Receptor T Cells. *Cancer Cell* 2019;35:221–37.
- Majzner RG, Theruvath JL, Nellan A, et al. CAR T Cells Targeting B7-H3, a Pan-Cancer Antigen, Demonstrate Potent Preclinical Activity Against Pediatric Solid Tumors and Brain Tumors. *Clin Cancer Res* 2019;25:2560–74.
- Vitanza NA, Wilson AL, Huang W, et al. Intraventricular B7-H3 CAR T Cells for Diffuse Intrinsic Pontine Glioma: Preliminary First-in-Human Bioactivity and Safety. *Cancer Discov* 2023;13:114–31.
- Cong F, Yu H, Gao X. Expression of CD24 and B7-H3 in breast cancer and the clinical significance. *Oncol Lett* 2017;14:7185–90.
- Hagelstein I, Wessling L, Rochwarger A, et al. Targeting CD276 for T cell-based immunotherapy of breast cancer. *J Transl Med* 2024;22:902.
- Lee DW, Ryu HS, Nikas IP, et al. Immune marker expression and prognosis of early breast cancer expressing HER3. *Eur J Cancer* 2024;213:115081.
- Wang X, Wang Y, Yu L, et al. CSPG4 in cancer: multiple roles. *Curr Mol Med* 2010;10:419–29.
- Cattaruzza S, Ozerdem U, Denzel M, et al. Multivalent proteoglycan modulation of FGF mitogenic responses in perivascular cells. *Angiogenesis* 2013;16:309–27.
- Pellegatta S, Savoldo B, Di Ianni N, et al. Constitutive and TNF α -inducible expression of chondroitin sulfate proteoglycan 4 in glioblastoma and neurospheres: Implications for CAR-T cell therapy. *Sci Transl Med* 2018;10:eaa02731.
- Geldres C, Savoldo B, Hoyos V, et al. T lymphocytes redirected against the chondroitin sulfate proteoglycan-4 control the growth of multiple solid tumors both in vitro and in vivo. *Clin Cancer Res* 2014;20:962–71.
- Wang X, Osada T, Wang Y, et al. CSPG4 protein as a new target for the antibody-based immunotherapy of triple-negative breast cancer. *J Natl Cancer Inst* 2010;102:1496–512.
- Hu Z-Y, Zheng C, Yang J, et al. Co-Expression and Combined Prognostic Value of CSPG4 and PDL1 in TP53-Aberrant Triple-Negative Breast Cancer. *Front Oncol* 2022;12:804466.
- Garcia-Recio S, Hinoue T, Wheeler GL, et al. Multiomics in primary and metastatic breast tumors from the AURORA US network finds

- microenvironment and epigenetic drivers of metastasis. *Nat Cancer* 2023;4:128–47.
- 31 Parker JS, Mullins M, Cheang MCU, *et al.* Supervised risk predictor of breast cancer based on intrinsic subtypes. *J Clin Oncol* 2009;27:1160–7.
 - 32 Huang K-L, Li S, Mertins P, *et al.* Proteogenomic integration reveals therapeutic targets in breast cancer xenografts. *Nat Commun* 2017;8:14864.
 - 33 Li S, Shen D, Shao J, *et al.* Endocrine-therapy-resistant ESR1 variants revealed by genomic characterization of breast-cancer-derived xenografts. *Cell Rep* 2013;4:1116–30.
 - 34 Landoni E, Fucá G, Wang J, *et al.* Modifications to the Framework Regions Eliminate Chimeric Antigen Receptor Tonic Signaling. *Cancer Immunol Res* 2021;9:441–53.
 - 35 Diaconu I, Ballard B, Zhang M, *et al.* Inducible Caspase-9 Selectively Modulates the Toxicities of CD19-Specific Chimeric Antigen Receptor-Modified T Cells. *Mol Ther* 2017;25:580–92.
 - 36 Vera J, Savoldo B, Vigouroux S, *et al.* T lymphocytes redirected against the kappa light chain of human immunoglobulin efficiently kill mature B lymphocyte-derived malignant cells. *Blood* 2006;108:3890–7.
 - 37 Ramos CA, Grover NS, Beaven AW, *et al.* Anti-CD30 CAR-T Cell Therapy in Relapsed and Refractory Hodgkin Lymphoma. *J Clin Oncol* 2020;38:3794–804.
 - 38 Ritchie ME, Phipson B, Wu D, *et al.* limma powers differential expression analyses for RNA-sequencing and microarray studies. *Nucleic Acids Res* 2015;43:e47.
 - 39 Foster MC, Savoldo B, Lau W, *et al.* Utility of a safety switch to abrogate CD19.CAR T-cell-associated neurotoxicity. *Blood* 2021;137:3306–9.
 - 40 Sun C, Shou P, Du H, *et al.* THEMIS-SHP1 Recruitment by 4-1BB Tunes LCK-Mediated Priming of Chimeric Antigen Receptor-Redirected T Cells. *Cancer Cell* 2020;37:216–25.
 - 41 Zhao Z, Condomines M, van der Stegen SJC, *et al.* Structural Design of Engineered Costimulation Determines Tumor Rejection Kinetics and Persistence of CAR T Cells. *Cancer Cell* 2015;28:415–28.
 - 42 Krug K, Jaehnig EJ, Satpathy S, *et al.* Proteogenomic Landscape of Breast Cancer Tumorigenesis and Targeted Therapy. *Cell* 2020;183:1436–56.
 - 43 Feucht J, Sun J, Eyquem J, *et al.* Calibration of CAR activation potential directs alternative T cell fates and therapeutic potency. *Nat Med* 2019;25:82–8.
 - 44 Haubner S, Mansilla-Soto J, Nataraj S, *et al.* Cooperative CAR targeting to selectively eliminate AML and minimize escape. *Cancer Cell* 2023;41:1871–91.
 - 45 Muliaditan T, Halim L, Whilding LM, *et al.* Synergistic T cell signaling by 41BB and CD28 is optimally achieved by membrane proximal positioning within parallel chimeric antigen receptors. *Cell Rep Med* 2021;2:100457.
 - 46 Majzner RG, Rietberg SP, Sotillo E, *et al.* Tuning the Antigen Density Requirement for CAR T-cell Activity. *Cancer Discov* 2020;10:702–23.
 - 47 Haas AR, Golden RJ, Litzky LA, *et al.* Two cases of severe pulmonary toxicity from highly active mesothelin-directed CAR T cells. *Mol Ther* 2023;31:2309–25.